A CMOS CAMERA-BASED SYSTEM FOR NON-CONTACT PULSE OXIMETRY IMAGING

K. Humphreys*, T. Ward* and C. Markham**

* Dept. of Electronic Engineering, National University of Ireland, Maynooth, Co. Kildare, Ireland
** Dept. of Computer Science, National University of Ireland, Maynooth, Co. Kildare, Ireland

khumphreys@eeng.nuim.ie

Abstract: In this paper a non-contact pulse oximetry imaging system is described. The system utilises a CMOS digital camera and near infrared (NIR) light emitting diodes operating in a reflection mode to simultaneously capture photoplethysmograph (PPG) signals at two wavelengths. The Modified Beer-Lambert Law is used to extrapolate tissue oxygenation from the PPG signals. Attention is drawn to the system's potential in applications such as the assessment and management of wounds.

Introduction

Pulse oximetry is the non-invasive measuring of arterial oxygen saturation [1, 2]. It is an important clinical tool for monitoring the health of patients during anaesthesia and recovery [3]. A typical clinical pulse oximeter probe consists of two light emitting diodes, one emitting near infrared (NIR) and the other red light, and a photo diode detector. The two diodes are alternately energised producing pulses of NIR and red light. By either transmission through or reflection from tissue the transmitted pulses of light are detected by the photodiode. The emitters and detector are housed in a plastic clamp, which is typically attached to a finger. The clamp serves to maintain good contact with the tissue and to shield the detector from ambient light sources. Tissue is relatively transparent to light at these wavelengths however haemoglobin, a respiratory protein found in red blood cells (erythrocytes), is a strong absorber of light in this band. During the cardiac cycle, at times of high pressure (systole), the combination of increased blood volume under the probe and the alignment of the erythrocytes such that their long axis is perpendicular to the direction of blood flow [1], cause an increase in light absorption and a corresponding decease in transmitted or reflected light detected by the photo diode. Plotting the detected light intensity with respect to time yields a photoplethysmograph (PPG) trace. Haemoglobin has different absorption spectra in the red and NIR bands depending on whether it is oxygenated (HbO) or deoxygenated (Hb). By capturing simultaneous PPG signals at two wavelengths the relative concentrations of Hb and HbO can be determined and the oxygen saturation calculated. This can be achieved either by use of the Modified Beer-Lambert Law or more commonly in clinical devices by using a lookup table to directly relate the ratio of received NIR and red light to oxygen saturation.

During anaesthesia pulse oximetry is used as an early indicator of cyanosis, however in addition to being employed as an indicator of gross oxygen deficiency in the blood, pulse oximetry is suitable to monitoring the health and viability of smaller areas of tissue. It has been shown to be capable of detecting peripheral vascular disease [4]. It has also been used to assess the viability of tissue during surgery and experimentally to discern between ischaemia from which tissue will recover and ischaemia from which tissue necrosis will result [5]. The value of pulse oximetry in each of these applications is that it provides an objective measure of blood perfusion and oxygen saturation. Without a pulse oximeter, assessing the level of cyanosis or ischaemia is entirely subjective and depends on the experience of the clinician, the condition of the patient and even the ambient lighting [6].

An area that stands to benefit from pulse oximetry is the assessment of wounds such as pressure ulcers, which result form prolonged ischaemia and poor circulation. The conditions of such wounds are currently evaluated using subjective scales. The ability to monitor the perfusion and oxygen saturation of established ulcers and areas at risk of developing pressure ulcers would provide a useful and objective clinical tool. Conventional pulse oximeters require direct contact with the tissue under investigation, which precludes their use in these applications. In addition a conventional pulse oximeter takes readings at one discrete location at a time.

In this paper a CMOS camera-based pulse oximetry imaging system is described that requires no contact with the tissue under investigation and is capable of monitoring the perfusion and oxygen saturation of an area of tissue. The signal processing and the principles of extracting the haemodynamic information from the resulting data using the Modified Beer-Lambert Law are described.

Materials and Methods

The system, which is depicted in Figure 1, consists of a CMOS camera and two arrays of NIR light emitting diodes (LED) that can be rotated to bring both arrays to shine on the same area. Two wavelengths of LED are used, 760 nm and 880 nm. The 760 nm diodes are just below the visible red portion of the spectrum.

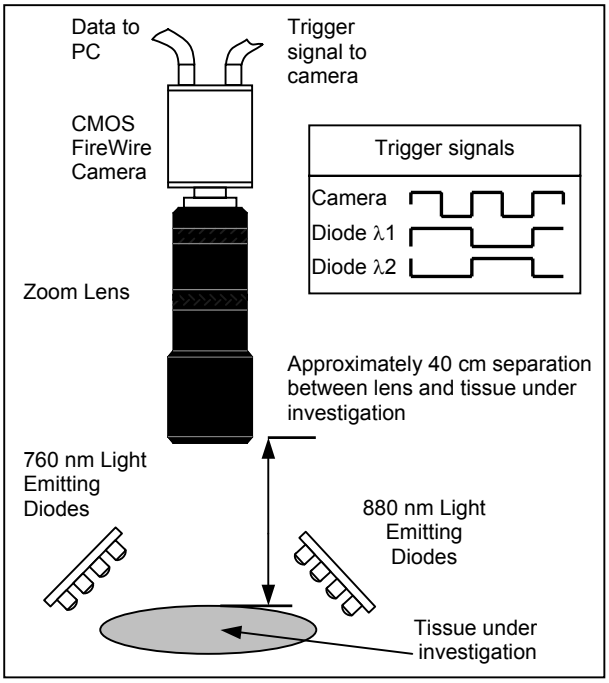

Figure 1: Depiction of pulse oximetry imaging system.

It is important that the two wavelengths lie either side of 800 nm, the isobestic point in the spectra of Hb and HbO where both have the same light absorption. The diodes used are metal cased with built in glass lenses with a FWHM beam angle of 8°. The 880 nm diodes emit 17 mW at a forward current 100 mA. The 760 nm diodes emit 10 mW at the same forward current. The camera (a monochromatic Pixelink PL-A741) uses a 2/3" CMOS sensor with 1280x1024 square pixels of length 6.7 μm and encodes pixels using either 8 or 10 bits. The camera has a sensitivity of 0.055 A/W at 880 nm and 0.091 A/W at 760 nm. It is connected to a PC via an IEEE 1394 FireWire connection. The camera is focused on the tissue under investigation by a zoom lens (focal length 18-108 mm, f2.5 to closed). Videos are recorded to the PC in uncompressed AVI format using a progressive scan. The diode arrays are alternately powered up and the camera is externally triggered to capture a frame when either array is powered up. A frame rate of 60 frames per second or 30 frames per wavelength per second provides an appropriate compromise between sampling often enough to capture the fine structure of the PPG signal while allowing a long enough exposure and read-out time for each frame. The camera is mounted on a tripod, with the lens face approximately 40 cm from the tissue under investigation. The diode arrays are positioned approximately 15 cm away from the tissue, such that they evenly illuminate an area of a few square centimetres. Since it is required to image a relatively small area the full spatial resolution of the camera is not required; selecting an area of 240x320 pixels in the middle of the CMOS chip provides sufficient spatial resolution while allowing for significantly higher frame rates.

Once a video has been recorded the resulting AVI file is split into frames captured at 880 nm and frames captured at 760 nm. Using Matlab, adjacent pixels in each frame are grouped together into boxes; the average pixel value of each box is found for each frame and plotted against time. The process is illustrated graphically in Figure 2 with data obtained by transmitting light through a subject's finger. By plotting the average value of the pixels in the white box in Figure 2(A) as they vary from frame to frame, the trace depicted in Figure 2(B) is obtained. This trace contains a distinct PPG signal in which the systolic and diastolic portions of the peripheral arterial waveform can be seen along with the dichrotic notch [7] (the inflection in the waveform associated with a momentary backflow of blood caused by the abrupt closure of the aortic valve).

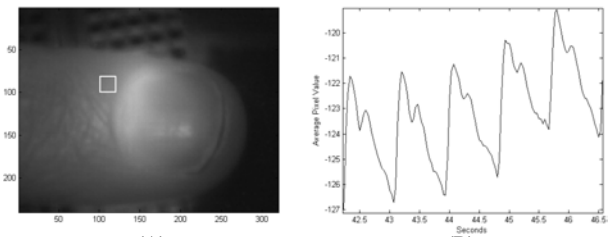

(A) (B)

Figure 2: (A) A sample frame with a 20x20 pixel box outlined. (B) Change in average pixel value of the box.

The process is performed on the set of frames associated with each wavelength and results in two PPG waveforms captured simultaneously at different wavelengths. It is then necessary to extrapolate from these data, the relative concentrations of the chromophores Hb and HbO, and hence the oxygen saturation. Two methods can be used. Conventional pulse oximeters employ a lookup table that relates the ratio of red to NIR light at the detector to percentage oxygen saturation (SpO_2) [1]. The approximate relationship is depicted in Figure 3.

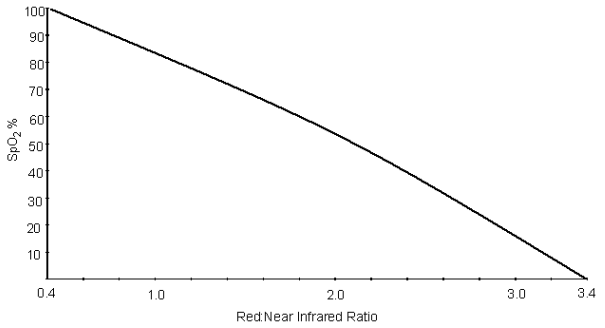

Figure 3: Approximate relationship between SpO_2 % and Red:NIR ratio.

The second method that can be used to calculate the SpO_2 value involves the application of simultaneous equations describing the Modified Beer-Lambert Law to solve for the relative concentrations of Hb and HbO.

The algorithm used here is based on that described in reference [8]. The Modified Beer-Lambert Law is described by (1).

$$A = \log_{10}(I_0 / I) = \alpha.c.d.B + G \qquad (1)$$

This law sates that the attenuation (A) measured at the detector as the logarithm of the incident light (I_0) divided by the detected light (I), is equal to the specific extinction coefficient of the absorbing substance (α), multiplied by the concentration (c) of that substance, multiplied by the distance between source and detector (d), multiplied by a differential path length factor (B). The B factor accounts for the fact that due to scattering a photon travels a much greater distance than the geometrical distance between source and detector. While scattering causes most photons to travel a longer path, it causes others to avoid the detector completely. An additional term is added to the expression to account for loss of photons due to scattering (G). The scattering loss is assumed to be constant for a given tissue. The effective path length ($d.B$) varies little and α is fixed for a specific absorber at any particular wavelength. Thus (assuming I_0 remains constant) by differentiating (1) with respect to time the equation reduces to that described in (2).

$$\Delta A = A_1 - A_2 = \log_{10}(I_2 - I_1) = \alpha.\Delta c.d.B \qquad (2)$$

The values of α, d and B are known for the absorbers and tissues in question, so by measuring the change in light attenuation at a particular wavelength, the change in concentration of the absorber can be determined. Since blood has two significant absorbers (Hb and HbO) the change in attenuation of light of wavelength 760 nm over time can be described by (3).

$$\Delta A_{760nm} /(B.d) = \alpha_{760nm,Hb}\Delta c_{Hb} + \alpha_{760nm,HbO_2}\Delta c_{HbO_2} \qquad (3)$$

Similarly the change at 880 nm is given by (4).

$$\Delta A_{880nm} /(B.d) = \alpha_{880nm,Hb}\Delta c_{Hb} + \alpha_{880nm,HbO_2}\Delta c_{HbO_2} \qquad (4)$$

This can be expressed in matrix form as $A/(Bd)=\alpha C$ and solved for C by finding the pseudo-inverse of α, such that $C=(\alpha^T\alpha)^{-1}\alpha A/(Bd)$ (where α^T is the transpose of α).

In the camera based system identifying the distance between the source and detector (d) requires some consideration. Although the actual distance between the diodes and camera is large, for most of that distance the photons are traveling through air. The appropriate length is the distance between the point where a photon enters the tissue and the location where the camera observes it leaving. The differential path length factor (B) has been shown to be both wavelength and age dependent [8]. The differential path length factor for 780 nm is given by B_{780}=5.13+0.07(age in years)$^{0.81}$. To obtain the value of B_{760} and B_{880}, the calculated value of B_{780} is scaled by a factor of 1.12 and 0.84 respectively as described in reference [8].

Results

Figure 4 depicts results obtained using the pulse oximetry imaging system. During the experiment the subject was seated in an upright position with their right forearm resting on a table with the palm of their hand facing upwards. The camera lens was focused on a small portion (approximately 4 cm^2) of the palm of the subject's hand. A video consisting of 1000 frames was recorded at a rate of 60 fps with an exposure time of 12 ms per frame. The video was processed using the method described in the previous section. The data in Figure 4 were taken from a 20x20 pixel box positioned in the centre of the video frame. The data are typical of pixel groups located in well-illuminated areas of the frame. No signal processing is applied other than the averaging of the pixel values in the group.

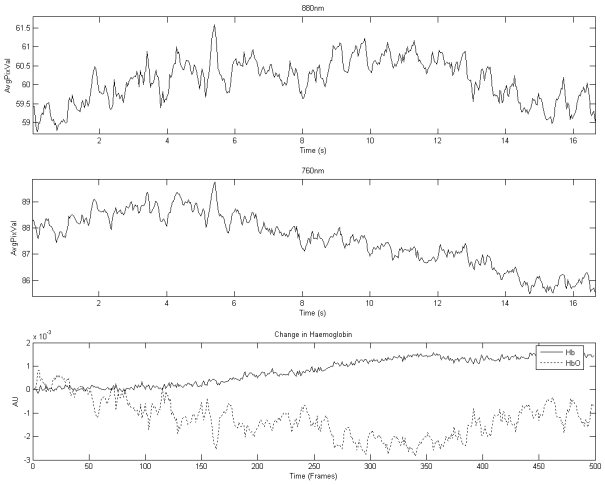

Figure 4: (Top) PPG signal captured at 880 nm, (middle) PPG captured at 760 nm and (bottom) corresponding changes in concentrations of Hb and HbO.

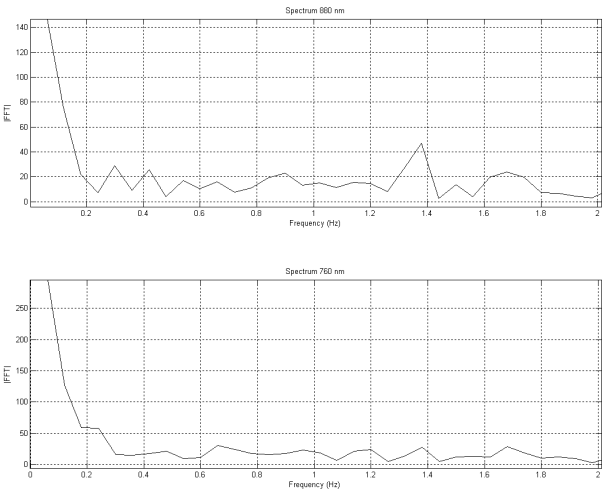

Figure 5: Frequency spectrum of data in Figure 4.

The data in Figure 4 appear noisy in comparison to conventional PPG signals, even in comparison to signals obtained using a camera in transmission mode [9], however a pulse component can be seen with duration of slightly less than 1 second. This can also be seen in Figure 5, which shows the spectra of the PPG signals in Figure 4. A peak can be seen in the spectra at a frequency of approximately 1.35 Hz. This corresponds to a heart rate of 81 beats per minute. During the experiment a conventional contact pulse oximeter (a Welch Allyn patient monitoring device attached to a Nelcor pulse oximeter probe) was attached to subject and measured the heart rate and SpO_2 values. The conventional device recorded a heart rate varying between 74 and 83 beats per minute, which correlates well with the camera based system. Also visible in the spectra is the effect of breathing at approximately 0.3 Hz and the effects of the low frequency vasomotion and Mayer wave at approximately 0.1 Hz and lower.

It can be seen in both the time domain plots of Figure 4 and the spectra in Figure 5 that the pulse is more pronounced in the 880 nm signal than the 760 nm signal. This is to be expected as tissue has a more diffusing affect at 760 nm, resulting in a weaker signal at the detector. In order to improve the signal to noise ratio of the data prior to calculating the SpO2, the data are first low pass filtered using a 2nd order Butterworth filter with a 5 Hz cut-off frequency. The filtered PPG signals can be seen in Figure 6.

Arterial oxygen saturation can be defined as the number of haemoglobin sites with oxygen molecules attached, divided by the total number of haemoglobin sites available for oxygen transportation as in (5).

$$SpO_2(\%) = \frac{HbO_2}{HbO_2 + Hb} \times 100 \qquad (5)$$

A percentage reading of SpO_2 can be calculated from the data presented in Figure 6 by comparing the corresponding pulse heights in the Hb and HbO

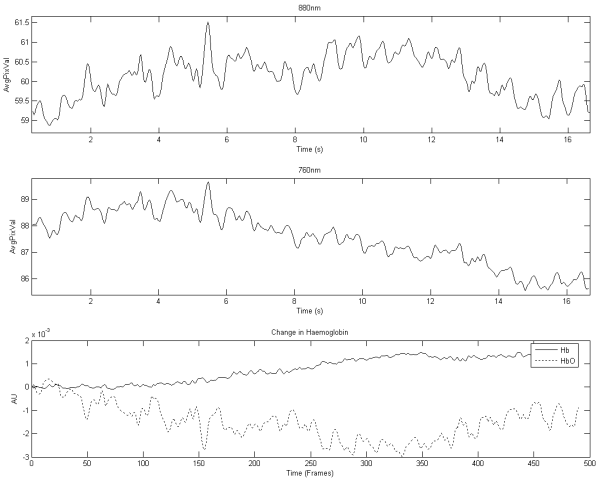

Figure 6: Low pass filtered PPG signals and corresponding change in Hb and HbO concentrations.

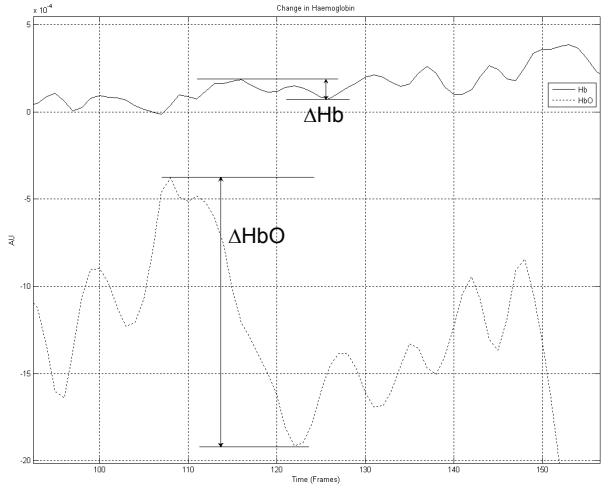

Figure 7: Calculation of SpO_2 from ΔHbO and ΔHb using equation (5). $1.54x10^{-3}/(1.54x10^{-3}+1.1x10^{-4})=93\%$

concentration change graphs and applying them to equation (5) as described in reference [10]. A sample calculation is illustrated in Figure 7, which results in an SpO2 value of 93%. Performing this calculation across the entire data set results in SpO_2 values from 88% to 98%. The actual value of the subject's arterial oxygen saturation during the experiment was measured by the conventional pulse oximeter at 98% for the duration.

Discussion

The sometimes-large deviation between the conventional pulse oximeter and the camera-based system can be attributed to several factors. Over time and with change in temperature, the emission characteristics of the diodes change. In addition the sensitivity of the CMOS sensor varies with wavelength. These factors were not incorporated into the calculations described above. The camera-based system is also inherently susceptible to interference from ambient sources of light, overhead lighting, monitors and daylight for example. In this respect the camera system's performance could be improved by the addition of a NIR filter or the incorporation of a dark frame in the triggering sequence, where only extraneous ambient light is measured. Though motion artefacts degrade a conventional sensor's readings they are an even greater problem in a non-contact system.

Ultimately a non-contact pulse oximetry imaging system for use in wound assessment will need to be capable of identifying and contrasting regions of tissue with high and low oxygen saturation. When NIR light enters tissue it becomes highly scattered, most photons are lost but some find their way to the detector and form part of the recorded signal. The physical separation between the source and detector has a large bearing on the likely path a photon has travelled to arrive at that point as well as how deep it is likely to have penetrated the tissue [11]. A functional pulse oximetry imaging system would need to incorporate such information

when identifying areas of high and low perfusion and oxygenation. It would also likely require a more sophisticated illumination scheme, capable of selectively illuminating specific areas of the tissue under investigation.

Conclusion

A CMOS camera-based pulse oximetry imaging system has been presented that requires no contact with the tissue under investigation. The system performs well in comparison to a conventional contact pulse oximeter probe, with the camera having sufficient sensitivity to the NIR band and being capable of sufficiently high frame rates to accurately capture the cardiac pulse at two wavelengths simultaneously. It is more common to encounter more sensitive, cooled and back-illuminated CCD sensors in spectroscopic imaging applications [12]. In general however these devices are not capable of the high frame rates needed to capture PPG signals at two wavelengths.

The system's oxygen saturation calculations are less accurate when compared to the conventional device. This has been attributed to the need for calibration of several factors, predominant among which is the intensity of the light sources.

The development of an adaptable illumination scheme capable of illuminating discrete areas of the tissue under investigation along with the thorough modelling of the NIR light in the tissue have been identified as necessary steps to developing a more practical oximetry imaging system.

References

[1] Moyle J., (1994): 'Pulse Oximitery', BMJ Publishing Group

[2] Wukitsch M., Petterson M., Tobler D., and Pologe J. (1988): 'Pulse oximitery: analysis of theory, technology and practice', *Journal of Clinical Monitoring*, **1988**, pp. 290-301

[3] Severinghaus J. and Astrup P. (1986): 'History of blood gas analysis', *Journal of Clinical Monitoring*, **2**, pp. 174-189

[4] Joyce W., Walsh K., Gough J., Gorey T., and Fitzpatrick J. (1990): 'Pulse oximetry: a new non-invasive assessment of peripheral arterial occulsive disease', *British Journal of Surgery*, **77**, pp. 115-117

[5] DeNobile J., Guzzetta P., and Patterson K. (1990): 'Pulse oximetry as a means of assessing bowel viability', *Journal of Surgical Research*, **48**, pp. 21-23

[6] Comroe J. and Botelho S. (1947): 'The unreliability of cyanosis in the recognition of arterial hypoxema', *American Journal of Medical Science*, **214**, pp. 1-6

[7] Humphreys K., Markham C., and Ward T. (2005): 'A CMOS camera-based system for clinical photoplethysmographic applications', *Proceedings of SPIE*, **5823**, pp. 88-95

[8] Cope M., *The development of a near infrared spectroscopy system and its application for non invasive monitoring of cereberal blood flow and tissue oxygenation in the newborn infant*, Ph.D., Department of Medical Physics and Bioengineering, University College London, 1991

[9] Humphreys K., Ward T., and Markham C. (2005): 'A CMOS camera-based pulse oximetry imaging system', 27th Annual International Conference of the IEEE Engineering in Medicine and Biology Society

[10] Rolfe P. (2000): 'In vivo near-infrared spectroscopy', *Biomedical Engineering Annual Review*, **2**, pp. 715-754

[11] Okada E., Firbank M., Schweiger M., Arridge S., Cope M., and Deply D. (1997): 'Theoretical and experimental investigation of the near-infrared light propagation in a model of the adult head', *Applied Optics*, **36**, pp. 21-31

[12] Attas M., Hewko M., Pologe J., Posthumus T., Sowa M., and Mantsch H. (2001): 'Visualization of cutaneous hemoglobin oxygenation and skin hydration using near-infrared spectroscopic imaging', *Skin Research and Technology*, **7**, pp. 238-245